HHS Public Access

Author manuscript

Stroke. Author manuscript; available in PMC 2022 July 01.

Published in final edited form as:

Stroke. 2021 July ; 52(7): 2393–2403. doi:10.1161/STROKEAHA.121.034173.

FTO participates in hemorrhage-induced thalamic pain by stabilizing toll-like receptor 4 expression in thalamic neurons

Ganglan Fu, MD[#], **Shibin Du, MD**[#], **Tianfeng Huang, MD**[#], **Minghui Cao, MD, PhD**[#], **Xiaozhou Feng, PhD**, **Shaogen Wu, MD, PhD**, **Sfian Albik, MD**, **Alex Bekker, MD, PhD**, **Yuan-Xiang Tao, MD, PhD**

Department of Anesthesiology, New Jersey Medical School, Rutgers, The State University of New Jersey, Newark, NJ 07103, USA

[#] These authors contributed equally to this work.

Abstract

Background and Purpose: Hemorrhage-caused gene changes in the thalamus likely contribute to thalamic pain genesis. RNA N^6-methyladenosine (m^6A) modification is an additional layer of gene regulation. Whether fat-mass and obesity-associated protein (FTO), an m^6A demethylase, participates in hemorrhage-induced thalamic pain is unknown.

Methods: Expression of *Fto* mRNA and protein was assessed in mouse thalamus after hemorrhage caused by microinjection of type IV collagenase (Coll IV) into unilateral thalamus. Effect of intraperitoneal administration of meclofenamic acid (MA; a FTO inhibitor) or microinjection of adeno-associated virus-5 expressing Cre (AAV5-*Cre*) into the thalamus of $Fto^{fl/fl}$ mice on the Coll IV microinjection-induced Toll-like receptor 4 (TLR4) upregulation and nociceptive hypersensitivity was examined. Effect of thalamic microinjection of AAV5 expressing *Fto* (AAV5-*Fto*) on basal thalamic TLR4 expression and nociceptive thresholds was also analyzed. Additionally, level of m^6A in *Tlr4* mRNA and its binding to FTO or YTH N^6-methyladenosine RNA binding protein 2 (YTHDF2) were observed.

Results: FTO was detected in neuronal nuclei of thalamus. Level of FTO protein, but not mRNA, was time-dependently increased in the ipsilateral thalamus on days 1-14 after Coll IV microinjection. Intraperitoneal injection of MA or AAV5-*Cre* microinjection into $Fto^{fl/fl}$ mouse thalamus attenuated the Coll IV microinjection-induced TLR4 upregulation and tissue damage in the ipsilateral thalamus and development and maintenance of nociceptive hypersensitivities on the contralateral side. Thalamic microinjection of AAV5-*Fto* increased TLR4 expression and elicited hypersensitivities to mechanical, heat and cold stimuli. Mechanistically, Coll IV microinjection produced an increase in FTO binding to *Tlr4* mRNA, an FTO-dependent loss of m^6A sites in *Tlr4* mRNA and a reduction in the binding of YTHDF2 to *Tlr4* mRNA in the ipsilateral thalamus.

Corresponding author: Yuan-Xiang Tao, M.D., Ph.D., Department of Anesthesiology, New Jersey Medical School, Rutgers, The State University of New Jersey, 185 S. Orange Ave., MSB, E-661, Newark, NJ 07103. Tel: +1-973-972-9812; Fax: +1-973-972-1644. yuanxiang.tao@njms.rutgers.edu, Twitter account for Yuan-Xiang Tao: @YuanXiangTao1, Facebook account for Yuan-Xiang Tao: /yuanxiang.tao.

Disclosures: None.

Conclusion: Our findings suggest that FTO participates in hemorrhage-induced thalamic pain by stabilizing TLR4 upregulation in thalamic neurons. FTO may be a potential target for the treatment of this disorder.

Keywords

FTO; TLR4; m^{6}A modification; thalamic pain; hemorrhagic stroke

Introduction

Stroke is a leading cause of disability or death among aging population[1]. It significantly impacts the patients' quality of life and leads to a marked economic burden to the patients' families. Although only about 8-18% of the strokes are caused by brain hemorrhage, the rate in mortality associated with hemorrhagic stroke is much higher than that after ischemic stroke[2]. Besides functional losses in cognition and locomotor after stroke, approximately 8-14% of hemorrhagic victims suffer from refractory central poststroke pain (CPSP)[3]. The treatments for CPSP are very limited as current medications are ineffective and/or produce severe side effects[4]. Therefore, understanding the mechanisms of how CPSP is caused may open a new avenue in the management of this disorder.

Following stroke, there were a large number of differentially expressed genes in brain[5, 6]. These dysregulated genes likely contribute to CPSP genesis. For example, toll-like receptor 4 (TLR4) was significantly increased in damaged brains after ischemia or hemorrhage[7]. Suppression or blockage of TLR4 improved brain damage and blocked mechanical allodynia after carotid artery occlusion[7, 8]. However, how these CPSP-associated genes are increased after stroke remains incompletely understood.

Recent studies indicate that the mechanism for gene regulation involves N6-methyladenosine (m^{6}A)-mediated RNA modification. The m^{6}A on RNAs is reversibly catalyzed by a protein complex (writers) including methyltransferase-like 3 and 14 (METTL3 and METTL14) and Wilms' tumor 1-associating protein (WTAP) and removed by two demethylases (erasers) fat-mass and obesity-associated protein (FTO) and AlkB homolog 5 (ALKBH5)[9]. RNA m^{6}A is specifically recognized by m^{6}A-bidning proteins (readers) such as YTH N^6-Methyladenosine RNA Binding Proteins 1/2/3 (YTHDF1/2/3), which mediates divergent roles of m^{6}A in the RNA metabolism[10-12]. In particular, YTHDF2 rapidly degrades its binding RNAs[13]. We recently reported that increased FTO contributes to nerve injury-induced nociceptive hypersensitivity through stabilizing G9a expression in injured neurons of dorsal root ganglion[11]. Whether FTO also participates in CPSP genesis is unknown. In the present study, we evaluated its role in hemorrhage-induced thalamic pain.

Methods

The data that support the findings of this study are available from the corresponding author upon reasonable request.

Animal preparation

The usage of adult (7-8 weeks) male CD1 mice and *Fto*$^{fl/fl}$ mice (C57BL/6J background) was approved by the Animal Care and Use Committee of Rutgers New Jersey Medical School (Protocol #: PROTO999900990). We adhered to the AHA Journals' implementation of the Transparency and Openness Promotion (TOP) Guidelines. Details are described in the Data Supplement.

Hemorrhage-Induced Thalamic Pain Model

Hemorrhage-induced thalamic pain was established as described in our previous reports[14]. Details are described in the Data Supplement.

Behavioral Tests

Mechanical, heat and cold tests as well as locomotor function test were carried out as described previously[15]. There was a one-hour interval between two tests. Details are described in the Data Supplement.

Cell Line Culture and Transfection

The CAD cells were cultured and transfected by the plasmids as described previously[15]. Details are described in the Data Supplement.

TUNEL Staining

Cell death was detected using an in situ cell death detection kit for terminal deoxynucleotidyl transferase-mediated deoxyuridine triphosphate nick end labeling (TUNEL, EMD Millipore). Details are described in the Data Supplement.

Real-Time Polymerase Chain Reaction

The levels of the RNAs were measured with the SYBR-green method. Single-cell real-time RT-PCR assay was carried out as described previously[15]. Details are described in the Data Supplement.

Plasmid Constructs and Virus Production

The pro-viral plasmids were constructed and the AAV5 particles were packaged as described previously[15]. Details are described in the Data Supplement.

Western Blotting and Immunofluorescence Analyses

Western Blotting and immunofluorescence were evaluated, as described previously[11, 14, 15]. The specificity of the primary antibodies used has been reported previously[11, 14, 16-18]. Details are described in the Data Supplement.

RNA Immunoprecipitation (RIP) Assay

The RIP assay was performed using the Magna RIP Kit or the Magna MeRIP™ m6A Kit (Upstate/ EMD Millipore). Details are described in the Data Supplement.

Statistical Analysis

Statistical analysis was performed by using Graph Pad Prism 8.0 or Microcal Origin 2019 software. Normality and variance homogeneity of the data were assessed across all groups by the Shapiro-Wilk test/D'Agostino K squared test and the Levene's test, respectively. Parametric data were presented as mean ± SD and nonparametric data were reported as median and interquartile range from at least 3 independent experiments. Parametric data were analyzed by two-tailed, unpaired Student's t test or a one-way or two-way ANOVA followed by the *post hoc* Tukey test for multiple comparisons, while nonparametric data were analyzed by Scheirer-Ray-Hare test. Differences were considered significant with a $P < 0.05$. Details are described in the Supplemental materials.

RESULTS

FTO is increased in the ipsilateral thalamus after thalamic hemorrhage

Unilateral microinjection of Coll IV, but not saline, produced significant and sustained mechanical allodynia, heat hyperalgesia and cold hyperalgesia, which occurred 1 day after microinjection and persisted for at least 14 days after microinjection on the contralateral (not ipsilateral) side (Supplemental Fig. IA-D). This microinjection increased the expression of FTO protein, but not METTL3, METTL14, WTAP, ALKBH5, YTHDF1 and YTHDF2 proteins, in the whole ipsilateral thalamus (Fig. 1A-C). Interestingly, basal expression of *Fto* mRNA in the ipsilateral thalamus was not significantly altered after Coll IV or saline microinjection during observation period (Fig. 1D).

Distribution pattern of FTO in the thalamus was also examined. The triple labeling assay revealed that FTO co-expressed with NeuN (a specific neuronal marker) in the nuclei (labeled by DAPI) of individual cells and was not detected in the cellular nuclei of GFAP (a marker for astrocyte)- or Iba1 (a marker for microglia)-labeled cells in the region around/ adjacent to the core of hemorrhagic lesions in VPM and VPL 7 days after Coll IV microinjection (Supplemental Fig. II and Fig. III). The number of FTO-labeled neurons in this thalamic region on day 7 post-Coll IV microinjection was increased by 2.66-fold as compared to that after saline microinjection (Fig. 1E).

Effect of pharmacological inhibition of FTO on the hemorrhage-induced thalamic pain and damage

Meclofenamic acid (MA; 1, 5 or 10 mg/kg; dissolved in PBS), a specific inhibitor of FTO[19, 20] or vehicle (PBS) were intraperitoneally administered 30 min before Coll IV or saline microinjection and once a day for five days in male CD1 mice. Mechanical allodynia, heat hyperalgesia and cold hyperalgesia were developed on the contralateral (but not ipsilateral) side of the vehicle plus Coll IV-treated group on days 1-5 after microinjection (Fig. 2A-E). These pain hypersensitivities were markedly ameliorated in the MA (10 mg/kg)

plus Coll IV-treated mice (Fig. 2A-C). MA's effects were dose-dependent (Supplemental Fig. IVA-D). Moreover, intraperitoneal administration of MA (10 mg/kg), but not vehicle, once a day for 5 days starting 1 day after Coll IV microinjection significantly mitigated these pain hypersensitivities on the contralateral (not ipsilateral) side on days 3 and 5 after Coll IV microinjection (Supplemental Fig. VA-D). All treated mice displayed normal locomotor activities (Supplementary Table I).

TUNEL staining were carried out for the hemorrhage-induced cell death after behavioral tests on day 5 post-microinjection. As shown in Supplementary Fig. VI, many TUNEL-positive cells in the ipsilateral VPL and VPM were seen in the Coll IV plus vehicle-treated group and none of them in the saline plus vehicle- or MA-treated groups. Number of TUNEL-positive cells was dramatically reduced in the ipsilateral VPL and VPM of the Coll IV plus MA-treated group as compared to that in the Coll IV plus vehicle-treated group (Supplementary Fig. VI). Many cells that are positive for Iba1, GFAP, NeuN or CD68 (a marker for microphages and monocytes) were detected in the ipsilateral VPL and VPM of the Coll IV plus MA-treated group (Supplementary Fig. VII).

Effect of genetic knockdown of thalamic FTO on the hemorrhage-induced thalamic pain and damage

A major limitation of systemic MA administration is the lack of anatomical and pharmacological specificity. To this end, we knocked down thalamic FTO through microinjection of AAV5-*Cre* into unilateral thalamic VPL and VPM of male *Fto*$^{fl/fl}$ mice 5 weeks before Coll IV or saline microinjection into same region (Supplementary Fig. VIIIA). AAV5-*Gfp* was used as a negative control. Consistent with the previous study[15], GFP-labeled AAV5 transfected predominantly into thalamic neurons, as GFP co-existed with NeuN, but not Iba1 and GFAP, in the region around/adjacent to the core of hemorrhagic lesions in the ipsilateral thalamus on day 7 post-Coll IV microinjection (Supplementary Fig. VIIIB). The Coll IV microinjection-induced increase in the level of FTO protein was significantly blocked in whole ipsilateral thalamus of the AAV5-*Cre*-pre-microinjected male *Fto*$^{fl/fl}$ mice 7 days after Coll IV microinjection (Fig. 3A). Unexpectedly, male *Fto*$^{fl/fl}$ mice pre-microinjected with AAV5-Cre failed to alter basal level of FTO protein in the ipsilateral thalamus 7 days after saline microinjection (Fig. 3A). In line with behavioral observations above, significant mechanical allodynia, heat hyperalgesia and cold hyperalgesia were seen on days 1, 3 and 7 post-Coll IV microinjection on the contralateral (not ipsilateral) side of the AAV5-*Gfp*-premicroinjected male *Fto*$^{fl/fl}$ mice (Fig. 3B-F). However, these pain hypersensitivities were markedly reduced in the Coll IV male *Fto*$^{fl/fl}$ mice pre-microinjected with AAV5-*Cre* (Fig. 3B-D). Similar behavioral responses were observed in the female *Fto*$^{fl/fl}$ mice (Supplementary Fig. IXA-G).

The effect of thalamic FTO knockdown on the Coll IV-induced hemorrhagic lesion was also examined. As expected, many TUNEL-positive cells were seen in the ipsilateral VPL and VPM of the AAV5-*Gfp*-treated Coll IV mice, whereas none of TUNEL-positive cells were detected in the same region of the saline plus AAV5-*Gfp*- or AAV5-*Cre*-treated groups (Supplementary Fig. X). Number of TUNEL-positive cells was markedly decreased in the

ipsilateral VPL and VPM of the AAV5-*Cre* plus Coll IV-treated *Fto*$^{fl/fl}$ mice as compared to that in the AAV5-*Gfp* plus Coll IV-treated *Fto*$^{fl/fl}$ mice (Supplementary Fig. X).

Thalamic overexpression of FTO led to thalamic pain symptoms

The effect of thalamic FTO overexpression through thalamic microinjection of AAV5 expressing full-length *Fto* mRNA (AAV5-*Fto*) into unilateral VPL and VPM on basal nociceptive thresholds in naive adult male mice was observed. AAV5-*Gfp* was used as a control. Dramatic increases in the amounts of FTO mRNA and protein were detected in the injected thalamus 5 weeks after AAV5-*Fto* microinjection as compared to those after AAV5-*Gfp* microinjection (Fig. 4A-B). Mice microinjected with AAV5-*Fto*, but not AAV5-*Gfp*, displayed significant increases in paw withdrawal frequencies in response to 0.07 g and 0.4 g von Frey filament stimuli and marked decreases in paw withdrawal latencies in response to thermal and cold stimuli on the contralateral (not ipsilateral) side (Fig. 4C-F; Supplementary Fig. XI). These nociceptive hypersensitivities occurred 3 weeks post-microinjection and persisted for at least 5 weeks (Fig. 4C-F), consistent with the 3–4 weeks lag period of AAV5 expression[15]. Intraperitoneally injection of MA at 10 mg/kg (not vehicle) once a day for 5 days starting 5 weeks after viral microinjection significantly blocked these nociceptive hypersensitivities on days 3 and 5 post-MA injection (Supplementary Fig. XII). As expected, systemic MA administration did not affect locomotor function (Supplementary Table I).

Increased FTO involves in the hemorrhage-induced TLR4 upregulation in the thalamus

Given that upregulated TLR4 in hemorrhagic brains contributed to mechanical allodynia after stroke[7, 8], we predicted that increased thalamic FTO might involve in this upregulation. Indeed, pre-microinjection of AAV5-*Cre*, but not AAV5-*Gfp*, significantly blocked the Coll IV microinjection-induced increases in the level of TLR4 protein in the ipsilateral thalamus of *Fto*$^{fl/fl}$ mice on day 7 post-Coll IV microinjection (Fig. 5A). Neither virus affected basal expression of TLR4 protein in the ipsilateral thalamus of *Fto*$^{fl/fl}$ mice on day 7 after saline microinjection (Fig. 5A). Consistently, thalamic overexpression of FTO in the AAV5-*Fto*-microinjected mice markedly increased the amount of TLR4 protein in the injected thalamus, as compared to that in the AAV5-*Gfp*-microinjected mice (Fig. 5B). Moreover, this increase could be abolished after intraperitoneal injection of MA (but not PBS) (Fig. 5C). Our single-cell RT-PCR assay showed co-expression of *Fto* mRNA and *Tlr4* mRNA in individual thalamic neurons (Fig. 5D). Collectively, these findings suggest that increased FTO directly participates in the hemorrhage-induced TLR4 upregulation in thalamic neurons.

Increased FTO is responsible for a loss of m^{6}A sites in *Tlr4* mRNA in the hemorrhagic thalamus

Finally, we examined how increased FTO participated in TLR4 upregulation in hemorrhagic thalamus. RIP assay showed that binding activity between FTO and 3'-untranslated region (UTR) of *Tlr4* mRNA after Coll IV microinjection was increased by 2.59-fold as compared to that after saline microinjection in the ipsilateral thalamus 7 days post-microinjection (Fig. 6A). As FTO functions as an "eraser" to remove m^{6}A on RNAs[9], we detected that Coll IV microinjection produced a decrease of m^{6}A sites in this *Tlr4* mRNA region by 40% of the value after saline microinjection in the ipsilateral thalamus of the AAV5-*Gfp*-treated

Fto$^{fl/fl}$ mice 7 days after microinjection (Fig. 6B). This decrease was completely rescued by blocking increased FTO through thalamic microinjection of AAV5-*Cre* in the ipsilateral thalamus of the *Fto*$^{fl/fl}$ mice 7 days after Coll IV microinjection (Fig. 6B). These findings suggest that FTO is required for the hemorrhage-induced loss of m^{6}A in *Tlr4* mRNA. Expectedly, the binding activity between YTHDF2 and *Tlr4* mRNA's 3-UTR from the ipsilateral thalamus on day 7 post-Coll IV microinjection was significantly reduced by 54% as compared to that post-saline microinjection (Fig. 6C). This reduction caused by increased FTO-induced loss of m^{6}A sites may promote the stabilization of *Tlr4* mRNA. To further support this conclusion, we examined the effect of increased FTO on the decay time of *Tlr4* mRNA in *in vitro* cell lines. When the transcription was halted with actinomycin D, the decay rate of *Tlr4* mRNA was much slower in the FTO-overexpressing cells as compared to that in naive cells (Fig. 6D-E). This effect could be diminished by blocking FTO overexpression in the cells co-transfected with the vector expressing *Fto* shRNA (Fig. 6D-E). Our results indicate that increased FTO may be responsible for a loss of m6A sites in *Tlr4* mRNA and then stabilize TLR4 upregulation in the thalamus under hemorrhagic conditions.

4. Discussion

Hemorrhage-induced thalamic pain is one of chronic, refractory clinical diseases. During the past decades, a numerous number of animal studies as well as clinical observations on this disorder have been carried out[21], but the mechanisms of how thalamic hemorrhage causes pain hypersensitivities are still elusive. The present study demonstrated that thalamic microinjection of Coll IV led to an increase in FTO protein expression in the ipsilateral thalamus and that this increase contributed to Coll IV microinjection-induced development and maintenance of pain hypersensitivity. These effects were mediated likely by stabilizing TLR4 upregulation in thalamic neurons. Our findings indicate that FTO may play a key role in hemorrhage-induced thalamic pain.

The present study revealed that FTO was expressed predominantly in the nuclei of thalamic neurons. This cellular distribution was consistent with previous reports that showed the localization of FTO mainly in the neuronal nuclei of dorsal root ganglion[11] and cortex[22]. Moreover, we reported that FTO protein increased in the region around/adjacent to the core of hemorrhagic lesion of the ipsilateral thalamus after Coll IV microinjection. Consistently, FTO was detected in a great number of the neurons in this region after Coll IV microinjection. Inconsistent with our observation, a previous study reported that FTO expression significantly decreased in the peri-infarct cortex after transient middle cerebral artery occlusion[22]. The reason for the difference in FTO expression between present study and this previous work is still unclear, but it might be related to distinct molecular pathophysiology between ischemia and hemorrhage[23-25]. Interestingly, *Fto* mRNA expression in thalamus was not altered after Coll IV microinjection during the observation period. This result suggests that thalamic *Fto* gene is activated at the translational level, but not at the transcriptional level, in response to hemorrhagic insults. How hemorrhage causes an increase in FTO protein in thalamus remains unknown, but this increase is likely related to the elevations in the stability and translational efficiency of *Fto* mRNA.

Increased FTO in the ipsilateral thalamus is required for the development and maintenance of Coll IV microinjection-induced pain hypersensitivities. This conclusion was demonstrated not only by pharmacological FTO inhibition through intraperitoneal MA injection but also by blocking increased thalamic FTO through microinjection of AAV5-*Cre* into the ipsilateral VPM and VPL of the *Fto*$^{fl/fl}$ mice. Systemic administration of MA likely acts directly on thalamic neurons, because the blood-brain barrier was disrupted or dysfunctional after the hemorrhage[26]. However, MA's effect on the neurons/cells of other tissues could not be ruled out. We also observed that Coll IV microinjection-caused thalamic damage was improved by thalamic FTO inhibition or knockdown, as less TUNEL-positive cells were detected and surviving neurons, microglia, astrocytes and microphages were identified in the VPM and VPL after systemic pre-administration of MA or thalamic pre-microinjection of AAV5-*Cre* in the *Fto*$^{fl/fl}$ mice. This observation indicates that FTO inhibition or knockdown protects partial neurons from the Coll IV microinjection-induced neuronal damage in the VPM and VPL. The detected microglia, astrocytes and microphages might be associated with hemorrhage-caused inflammatory responses[14, 27]. We noticed that FTO genetic knockdown effect was less strong than systemic MA's effect. This may be attributed to the limitation in the microinjected volume of virus (0.5 μl). Additionally, both pharmacological inhibition and genetic knockdown of thalamic FTO profoundly attenuated, but not abolished, the Coll IV microinjection-induced pain hypersensitivities and thalamic damage. These partial effects may be related to the complicated and multiple mechanisms underlying the induction and maintenance of hemorrhage-induced thalamic pain. It is well documented that the excessive activation of excitatory postsynaptic glutamate receptors by increased synaptic release of glutamate and subsequently extreme Ca^{2+} influx into thalamic neurons through these receptors after hemorrhage contribute to thalamic pain genesis[21]. We recently reported that the expression of Fgr, a member of the Src family nonreceptor tyrosine kinases, was increased in thalamic microglia after hemorrhage and that this increase was involved in hemorrhage-induced thalamic pain[14]. Thus, combined strategies that target distinct mechanisms underlying thalamic hemorrhage-induced pain hypersensitivities may achieve great benefits in the management of this disorder.

Upregulated TLR4 in thalamic neurons may mediate the role of thalamic increased FTO in hemorrhage-induced thalamic pain. TLR4 was upregulated in ischemic or hemorrhagic brains[7]. Suppression or blockage of TLR4 improved brain damage and blocked mechanical allodynia after carotid artery occlusion[7]. TLR4 deficient mice displayed impaired peripheral neuropathic pain[28]. Activation of TLR4 led to the release of pro-inflammatory cytokines[29]. The latter activated microglia and vascular endothelial cells, increased cyclooxygenase, triggered apoptotic signaling pathways, contributed to intracerebral hemorrhagic development and provoked pain[29]. The evidence suggests that TLR4 is a critical initiator in the hemorrhage-induced thalamic pain. The present study found that increased FTO removed m^6A sites in *Tlr4* mRNA, leading to a loss in the binding of *Tlr4* mRNA to YTHDF2 in the ipsilateral thalamus after Coll IV microinjection. Given that YTHDF2 rapidly degrades its binding RNAs[30], increased FTO likely stabilized the hemorrhage-induced TLR4 upregulation in thalamic neurons. Indeed, FTO overexpression delayed the degradation of *Tlr4* mRNA in *in vitro* cell line. Blocking the Coll IV microinjection-induced thalamic FTO increase abolished the Coll IV microinjection-induced

TLR4 upregulation in the ipsilateral thalamus. Mimicking this increase elevated the level of TLR4 in the thalamus. Moreover, this elevation could be attenuated by FTO pharmacological inhibition. Given that *Fto* mRNA co-expressed with *Tlr4* mRNA in individual thalamic neurons, the anti-nociception caused by pharmacological inhibition or genetic knockdown of increased thalamic FTO likely results from destabilizing the Coll IV microinjection-induced TLR4 upregulation in the ipsilateral thalamic neurons. However, other potential mechanisms by which FTO participates in hemorrhage-induced thalamic pain cannot be ruled out. Using m^{6}A-eCLIP assay, our previous study revealed a loss and/or gain of m^{6}A sites in thousands of transcripts in injured dorsal root ganglion after peripheral nerve injury[11]. Thus, FTO contributes to hemorrhage-induced thalamic pain likely through its triggered multiple mechanisms, which merit to be further investigated in the future.

In conclusion, this study, to our knowledge, is the first time in providing the evidence that pharmacological inhibition or genetic knockdown of thalamic increased FTO attenuates the hemorrhage-induced thalamic pain without altering locomotor function and basal or acute pain. Considering that MA was approved by FDA in humans for use as a nonsteroidal anti-inflammatory drug and displays a favorable safety profile in patients[20], FTO may be a promising therapeutic target in the management of hemorrhage-induced thalamic pain.

Supplementary Material

Refer to Web version on PubMed Central for supplementary material.

Acknowledgements:

The authors thank Dr. Rudolph L. Leibel at Columbia University for providing *Fto*$^{fl/fl}$ mice and Dr. Virgil Muresan at Rutgers New Jersey Medical School for providing the CAD cells.

Funding Sources:

This work was supported by the grants (NS111553, NS094664, and NS113881) from the National Institutes of Health (Bethesda, Maryland, USA).

Non-standard Abbreviations and Acronyms

AAV5-*Cre*	adeno-associated virus 5 expressing Cre
AAV5-*Fto*	adeno-associated virus 5 expressing FTO
AAV5-*Gfp*	adeno-associated virus 5 expressing GFP
ALKBH5	AlkB homolog 5
Coll IV	type IV collagenase
CPSP	central poststroke pain
FTO	fat-mass and obesity-associated protein
GFP	green fluorescent protein
M^{6}A	N^6-methyladenosine

MA	meclofenamic acid
METTL3	methyltransferase-like 3
METTL14	methyltransferase-like 14
PCR	polymerase chain reaction
RIP	RNA immunoprecipitation
RT-PCR	real-time polymerase chain reaction
TLR4	toll-like receptor 4
TUNEL	terminal deoxynucleotidyl transferase-mediated deoxyuridine triphosphate nick end labeling
VPM	ventral posterior medial nuclei
VPL	ventral posterior lateral nuclei
WTAP	Wilms' tumor 1-associating protein
YTHDF1	YTH N^6-methyladenosine RNA binding protein 1
YTHDF2	YTH N^6-methyladenosine RNA binding protein 2

References

(1). Virani SS, Alonso A, Benjamin EJ, Bittencourt MS, Callaway CW, Carson AP, Chamberlain AM, Chang AR, Cheng S, Delling FNet al.Disease and Stroke Statistics-2020 Update: A Report From the American Heart Association. Circulation2020;141:e139–e596. [PubMed: 31992061]

(2). Feigin VL, Lawes CM, Bennett DA, Anderson CS. Stroke epidemiology: a review of population-based studies of incidence, prevalence, and case-fatality in the late 20th century. Lancet Neurol2003;2:43–53. [PubMed: 12849300]

(3). Kumar G, Soni CR. Central post-stroke pain: current evidence. J Neurol Sci2009;284:10–7. [PubMed: 19419737]

(4). Mulla SM, Wang L, Khokhar R, Izhar Z, Agarwal A, Couban R, Buckley DN, Moulin DE, Panju A, Makosso-Kallyth Set al.Management of Central Poststroke Pain: Systematic Review of Randomized Controlled Trials. Stroke2015;46:2853–60. [PubMed: 26359361]

(5). Hori M, Nakamachi T, Rakwal R, Shibato J, Nakamura K, Wada Y, Tsuchikawa D, Yoshikawa A, Tamaki K, Shioda S. Unraveling the ischemic brain transcriptome in a permanent middle cerebral artery occlusion mouse model by DNA microarray analysis. Dis Model Mech2012;5:270–83. [PubMed: 22015461]

(6). Dergunova LV, Filippenkov IB, Stavchansky VV, Denisova AE, Yuzhakov VV, Mozerov SA, Gubsky LV, Limborska SA. Genome-wide transcriptome analysis using RNA-Seq reveals a large number of differentially expressed genes in a transient MCAO rat model. BMC Genomics2018;19:655. [PubMed: 30185153]

(7). Hou Y, Zhang Y, Mi Y, Wang J, Zhang H, Xu J, Yang Y, Liu J, Ding L, Yang Jet al.A Novel Quinolyl-Substituted Analogue of Resveratrol Inhibits LPS-Induced Inflammatory Responses in Microglial Cells by Blocking the NF-kappaB/MAPK Signaling Pathways. Mol Nutr Food Res2019;63:e1801380. [PubMed: 31378007]

(8). Matsuura W, Harada S, Liu K, Nishibori M, Tokuyama S. Evidence of a role for spinal HMGB1 in ischemic stress-induced mechanical allodynia in mice. Brain Res2018;1687:1–10. [PubMed: 29476751]

(9). Yang Y, Hsu PJ, Chen YS, Yang YG. Dynamic transcriptomic m(6)A decoration: writers, erasers, readers and functions in RNA metabolism. Cell Res2018;28:616–24. [PubMed: 29789545]

(10). Albik S, Tao YX. Emerging role of RNA m6A modification in chronic pain. Pain: Janunary25, 2012 - Volume Articles in Press-Issue-doi: 10.1097/j.pain.0000000000002219.

(11). Li Y, Guo X, Sun L, Xiao J, Su S, Du S, Li Z, Wu S, Liu W, Mo Ket al.N(6)-Methyladenosine Demethylase FTO Contributes to Neuropathic Pain by Stabilizing G9a Expression in Primary Sensory Neurons. Adv Sci (Weinh)2020 ;7:1902402. [PubMed: 32670741]

(12). Zheng BX, Malik A, Xiong M, Bekker A, Tao YX. Nerve trauma-caused downregulation of opioid receptors in primary afferent neurons: Molecular mechanisms and potential managements. Exp Neurol2021;337:113572. [PubMed: 33340498]

(13). Wang X, Lu Z, Gomez A, Hon GC, Yue Y, Han D, Fu Y, Parisien M, Dai Q, Jia G, et al.N6-methyladenosine-dependent regulation of messenger RNA stability. Nature2014;505:117–20. [PubMed: 24284625]

(14). Huang T, Fu G, Gao J, Zhang Y, Cai W, Wu S, Jia S, Xia S, Bachmann T, Bekker A, Tao YX. Fgr contributes to hemorrhage-induced thalamic pain by activating NF-kappaB/ERK1/2 pathways. JCI Insight2020;5:e139987.

(15). Li Z, Mao Y, Liang L, Wu S, Yuan J, Mo K, Cai W, Mao Q, Cao J, Bekker Aet al.The transcription factor C/EBPbeta in the dorsal root ganglion contributes to peripheral nerve trauma-induced nociceptive hypersensitivity. Sci Signal2017;10:eaam5345. [PubMed: 28698219]

(16). Hess ME, Hess S, Meyer KD, Verhagen LA, Koch L, Bronneke HS, Dietrich MO, Jordan SD, Saletore Y, Elemento Oet al.The fat mass and obesity associated gene (Fto) regulates activity of the dopaminergic midbrain circuitry. Nat Neurosci2013;16:1042–8. [PubMed: 23817550]

(17). Li L, Zang L, Zhang F, Chen J, Shen H, Shu L, Liang F, Feng C, Chen D, Tao Het al.Fat mass and obesity-associated (FTO) protein regulates adult neurogenesis. Hum Mol Genet2017;26:2398–411. [PubMed: 28398475]

(18). Tian X, Zhu H, Du S, Zhang XQ, Lin F, Ji F, Tsou YH, Li Z, Feng Y, Ticehurst Ket al.Injectable PLGA-Coated Ropivacaine Produces A Long-Lasting Analgesic Effect on Incisional Pain and Neuropathic Pain. J Pain2021;22:180–95. [PubMed: 32739615]

(19). Chen B, Li Y, Song R, Xue C, Xu F. Functions of RNA N6-methyladenosine modification in cancer progression. Mol Biol Rep2019;46:2567–75. [PubMed: 30911972]

(20). Huang Y, Yan J, Li Q, Li J, Gong S, Zhou H, Gan J, Jiang H, Jia GF, Luo Cet al.Meclofenamic acid selectively inhibits FTO demethylation of m6A over ALKBH5. Nucleic Acids Res2015;43:373–84. [PubMed: 25452335]

(21). Dydyk AM, Munakomi S. Thalamic Pain Syndrome. In: StatPearls [Internet]. Treasure Island (FL): StatPearls Publishing; 20211.

(22). Chokkalla AK, Mehta SL, Kim T, Chelluboina B, Kim J, Vemuganti R. Transient Focal Ischemia Significantly Alters the m(6)A Epitranscriptomic Tagging of RNAs in the Brain. Stroke2019;50:2912–21. [PubMed: 31436138]

(23). Khoshnam SE, Winlow W, Farzaneh M, Farbood Y, Moghaddam HF. Pathogenic mechanisms following ischemic stroke. Neurol Sci2017;38:1167–86. [PubMed: 28417216]

(24). Righy C, Bozza MT, Oliveira MF, Bozza FA. Molecular, Cellular and Clinical Aspects of Intracerebral Hemorrhage: Are the Enemies Within?Curr Neuropharmacol2016;14:392–402. [PubMed: 26714583]

(25). Aronowski J, Zhao X. Molecular pathophysiology of cerebral hemorrhage: secondary brain injury. Stroke2011;42:1781–6. [PubMed: 21527759]

(26). Nadeau CA, Dietrich K, Wilkinson CM, Crawford AM, George GN, Nichol HK, Colbourne F. Prolonged Blood-Brain Barrier Injury Occurs After Experimental Intracerebral Hemorrhage and Is Not Acutely Associated with Additional Bleeding. Transl Stroke Res2019;10:287–97. [PubMed: 29949086]

(27). Hiraga SI, Itokazu T, Hoshiko M, Takaya H, Nishibe M, Yamashita T. Microglial depletion under thalamic hemorrhage ameliorates mechanical allodynia and suppresses aberrant axonal sprouting. JCI Insight2020;5:e131801.

(28). Tanga FY, Nutile-McMenemy N, DeLeo JA. The CNS role of Toll-like receptor 4 in innate neuroimmunity and painful neuropathy. Proc Natl Acad Sci U S A2005;102:5856–61. [PubMed: 15809417]

(29). Teng W, Wang L, Xue W, Guan C. Activation of TLR4-mediated NFkappaB signaling in hemorrhagic brain in rats. Mediators Inflamm2009;2009:473276. [PubMed: 20150961]

(30). Du H, Zhao Y, He J, Zhang Y, Xi H, Liu M, Ma J, Wu L. YTHDF2 destabilizes m(6)A-containing RNA through direct recruitment of the CCR4-NOT deadenylase complex. Nat Commun2016;7:12626. [PubMed: 27558897]

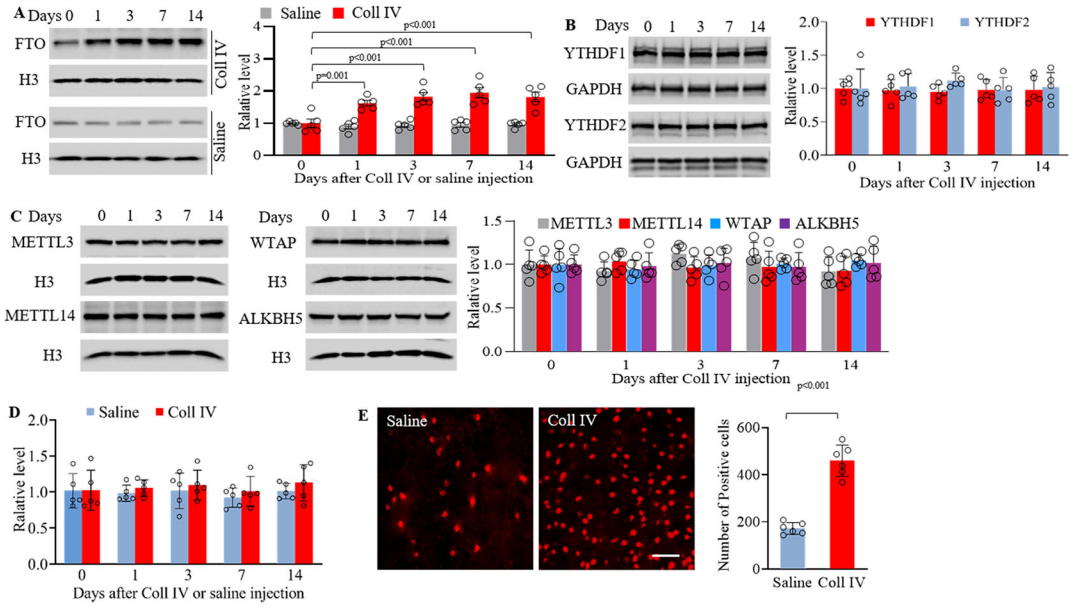

Figure 1.

Thalamic FTO protein was increased in collagenase IV (Coll IV)-induced thalamic pain model in male mice. (A) Level of FTO protein in the ipsilateral thalamus at different days after saline or Coll IV microinjection. n = 5 mice/group/time point. Statistical significance was calculated with two-way ANOVA (model × time) followed by *post hoc* Tukey test. $F_{model\ (1,\ 40)} = 111.597$, $p < 0.001$; $F_{time\ (4,\ 40)} = 6.031$, $p < 0.001$; $F_{model \times time\ (4,\ 40)} = 7.403$, $p < 0.001$. (B, C) Expression of YTHDF1, YTHDF2, METTL3, METTLE14, WTAP and ALKBH5 in the ipsilateral thalamus at different days after Coll IV microinjection. n = 5 mice/time point. Statistical significance was calculated with one-way ANOVA followed by *post hoc* Tukey test. YTHDF1: $F_{(4,\ 20)} = 0.0694$, $p = 0.991$. YTHDF2: $F_{(4,\ 20)} = 0.344$, $p = 0.845$. METTL3: $F_{(4,\ 20)} = 1.881$, $p = 0.153$. METTL14: $F_{(4,\ 20)} = 0.425$, $p = 0.789$. WTAP: $F_{(4,\ 20)} = 0.503$, $p = 0.734$. ALKBH5: $F_{(4,\ 20)} = 0.1$, $p = 0.981$. (D) Level of *Fto* mRNA in the ipsilateral thalamus at different days after Coll IV or saline microinjection. n = 5 mice/group/time point. Statistical significance was calculated with two-way ANOVA (model × time) followed by post hoc Tukey test. $F_{model\ (1,\ 40)} = 1.664$, $p = 0.205$; $F_{time\ (4,\ 40)} = 0.429$, $p = 0.787$; $F_{model \times time\ (4,\ 40)} = 0.103$, $p = 0.981$. (E) Number of the cells labeled by FTO in the ipsilateral thalamus 7 days after Coll IV or saline microinjection. n = 5 mice/group. Statistical significance was calculated with two-tailed unpaired Student's *t*-test. $t_{(10)} = 10.035$. Scale bar: 50 μm.

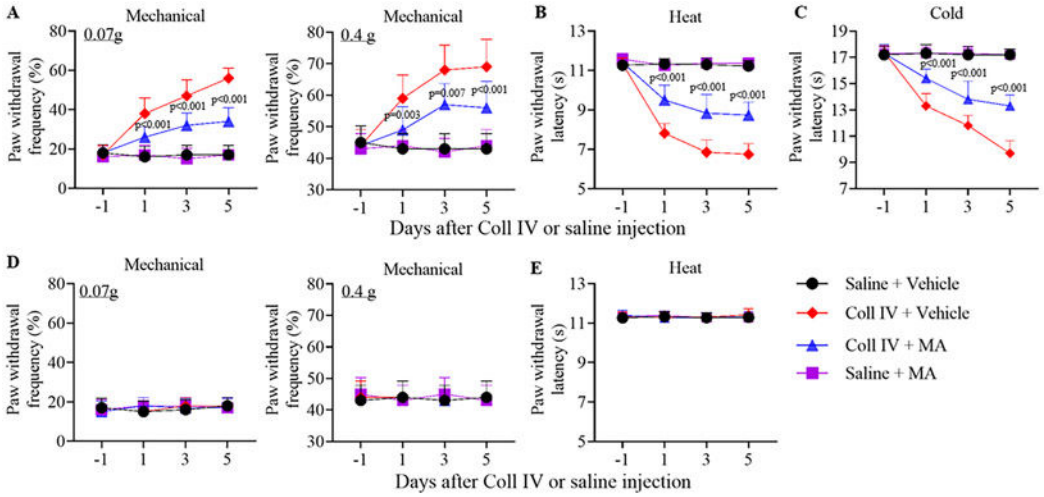

Figure 2.

Effect of intraperitoneal administration of meclofenamic acid (MA) on Coll IV microinjection-induced thalamic pain development in male mice. MA (10 mg/kg) or vehicle was given 30 min before microinjection and once daily for 5 days post-microinjection. Paw withdrawal frequencies to 0.07 g and 0.4 g von Frey filaments (A, D) and paw withdrawal latencies to heat (B, E) and cold (C) stimuli were examined on days 1, 3 and 5 after microinjection on the contralateral (A-C) and ipsilateral (D, E) sides. n = 10 mice/group. The *p* values on top of blue triangles indicate a difference between the vehicle and MA groups in Coll IV mice at the corresponding time points. Statistical significance was calculated with two-way ANOVA (time × treatment) with repeated measures followed by *post hoc* Tukey test. (A) For 0.07 g, $F_{time\ (3,\ 144)} = 43.958$, $p < 0.001$; $F_{treatment\ (3,\ 144)} = 150.666$, $p < 0.001$; $F_{time \times treatment\ (9,\ 144)} = 20.398$, $p < 0.001$. For 0.4 g, $F_{time\ (3,\ 144)} = 15.887$, $p < 0.001$; $F_{treatment\ (3,\ 144)} = 57.782$, $p < 0.001$; $F_{time \times treatment\ (9,\ 144)} = 7.951$, $p < 0.001$. (B) $F_{time\ (3,\ 144)} = 160.778$, $p < 0.001$; $F_{treatment\ (3,\ 144)} = 419.651$, $p < 0.001$; $F_{time \times treatment\ (9,\ 144)} = 48.742$, $p < 0.001$. (C) $F_{time\ (3,\ 144)} = 120.155$, $p < 0.001$; $F_{treatment\ (3,\ 144)} = 307.617$, $p < 0.001$; $F_{time \times treatment\ (9,\ 144)} = 46.073$, $p < 0.001$. (D) For 0.07 g, $F_{time\ (3,\ 144)} = 0.63$, $p = 0.597$. $F_{treatment\ (3,\ 144)} = 0.185$, $p = 0.906$; $F_{time \times treatment\ (9,\ 144)} = 0.704$, $p = 0.705$. For 0.4 g, $F_{time\ (3,\ 144)} = 0.0652$, $p = 0.978$; $F_{treatment\ (3,\ 144)} = 0.0652$, $p = 0.978$; $F_{time \times treatment\ (9,\ 144)} = 0.261$, $p = 0.984$. (E) $F_{time\ (3,\ 144)} = 0.373$, $p = 0.772$. $F_{treatment\ (3,\ 144)} = 0.351$, $p = 0.788$; $F_{time \times treatment\ (9,\ 144)} = 0.568$, $p = 0.822$.

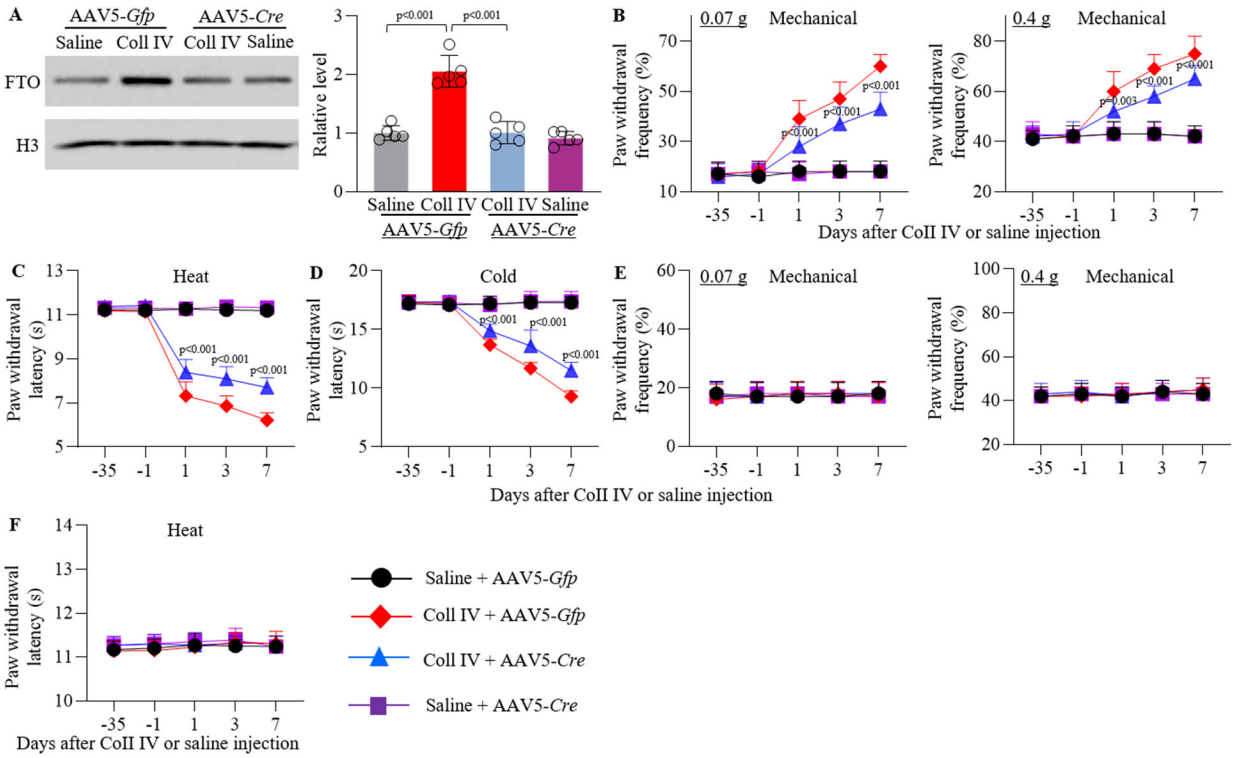

Figure 3.

Effect of thalamic pre-microinjection of AAV5-*Cre* on Coll IV microinjection-induced FTO protein expression and thalamic pain genesis in male *Fto*$^{fl/fl}$ mice. (A) Representative Western blots (left) and statistical summary of the densitometric analysis (right) on day 7 post-Coll IV or saline microinjection. n = 5 mice/group. Statistical significance was calculated with two-way ANOVA (treatment × model) followed by post hoc Tukey test. $F_{treatment\ (1,\ 16)} = 45.678$, $p < 0.001$; $F_{model\ (1,\ 16)} = 46.617$, $p < 0.001$; $F_{treatment \times model\ (1,\ 16)} = 32.469$, $p < 0.001$. (B-F) Paw withdrawal frequencies to 0.07 g and 0.4 g von Frey filaments (B, E) and paw withdrawal latencies to heat (C, F) and cold (D) stimuli on the contralateral (B-D) and ipsilateral (E, F) sides on days −35, 1, 3 and 7 after Coll IV or saline microinjection. n = 10 mice/group. The *p* values on top of blue triangles indicate a difference between the AAV5-*Gfp* and AAV5-*Cre* groups in Coll IV-microinjected mice at the corresponding time points. Statistical significance was calculated with two-way ANOVA (treatment × time) with repeated measures followed by *post hoc* Tukey test. (B) For 0.07 g, $F_{treatment\ (3,\ 180)} = 140.742$, $p < 0.001$; $F_{time\ (4,\ 180)} = 81.826$, $p < 0.001$; $F_{treatment \times time\ (12,\ 180)} = 27.861$, $p < 0.001$. For 0.4 g, $F_{treatment\ (3,\ 180)} = 110.388$, $p < 0.001$; $F_{time\ (4,\ 180)} = 65.624$, $p < 0.001$; $F_{treatment \times time\ (12,\ 180)} = 22.932$, $p < 0.001$. (C) $F_{treatment\ (3,\ 180)} = 410.233$, $p < 0.001$; $F_{time\ (4,\ 180)} = 198.524$, $p < 0.001$; $F_{treatment \times time\ (12,\ 180)} = 68.038$, $p < 0.001$. (D) $F_{treatment\ (3,\ 180)} = 201.154$, $p < 0.001$; $F_{time\ (4,\ 180)} = 117.912$, $p < 0.001$; $F_{treatment \times time\ (12,\ 180)} = 44.077$, $p < 0.001$. (E) For 0.07 g, $F_{treatment\ (3,\ 180)} = 0.063$, $p = 0.979$; $F_{time\ (4,\ 180)} = 0.155$, $p = 0.961$; $F_{treatment \times time\ (12,\ 180)} = 0.202$, $p = 0.998$. For 0.4 g, $F_{treatment\ (3,\ 180)} = 0.322$, $p = 0.809$; $F_{time\ (4,\ 180)} = 1.021$, $p = 0.398$; $F_{treatment \times time\ (12,\ 180)} = 0.23$, $p = 0.997$. (F) $F_{treatment\ (3,\ 180)} = 1.694$, $p = 0.17$; $F_{time\ (4,\ 180)} = 1.489$, $p = 0.207$; $F_{treatment \times time\ (12,\ 180)} = 0.503$, $p = 0.911$.

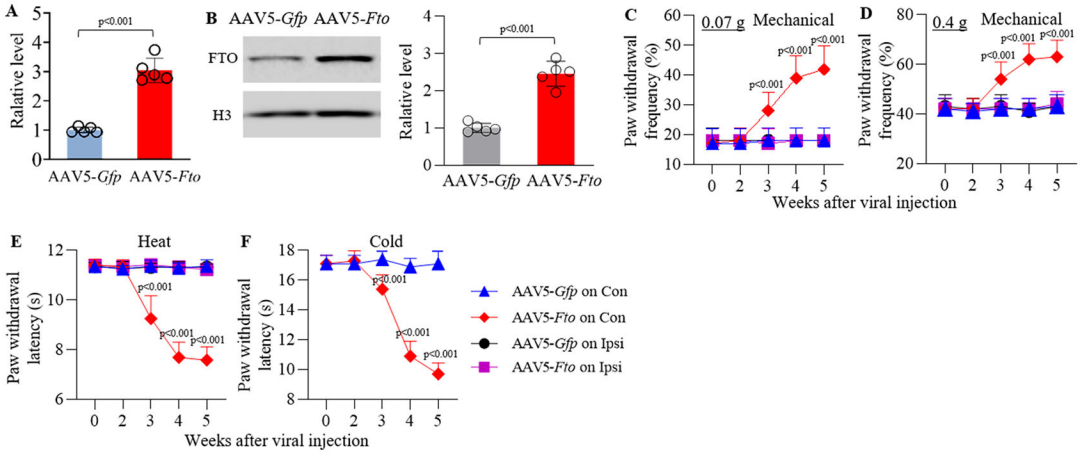

Figure 4.

Effect of thalamic FTO overexpression through AAV5-*Fto* microinjection into unilateral thalamus on nociceptive thresholds in naïve male mice. (A-B) Levels of *Fto* mRNA (A) and FTO protein (B) in the ipsilateral thalamus 5 weeks after viral microinjection. n = 5 mice/group/assay. Statistical significance was calculated with two-tailed, independent Student's *t* test. $t_{(8)} = -10.509$ in A and −8.993 in B. (C-F) Paw withdrawal frequencies to 0.07 g (C) and 0.4 g (D) von Frey filament stimuli and paw withdrawal latencies to thermal (E) and cold stimuli (F) on both ipsilateral (Ipsi) and contralateral (Con) sides at the different weeks after microinjection. n = 10 mice/group. The *p* values on top of red diamonds indicate a difference from the baseline (0 w) of the corresponding group. Statistical significance was calculated with two-way ANOVA (treatment × time) with repeated measures followed by *post hoc* Tukey test. (C) Con: $F_{treatment\ (1,\ 90)} = 105.313$, $p < 0.001$; $F_{time\ (4,\ 90)} = 24.397$, $p < 0.001$; $F_{treatment \times time\ (4,\ 90)} = 20.603$, $p < 0.001$. Ipsi: $F_{treatment\ (1,\ 90)} = 0.0545$, $p = 0.816$; $F_{time\ (4,\ 90)} = 0.0545$, $p = 0.994$; $F_{treatment \times time\ (4,\ 90)} = 0.0545$, $p = 0.994$. (D) Con: $F_{treatment\ (1,\ 90)} = 109.442$, $p < 0.001$; $F_{time\ (4,\ 90)} = 22.753$, $p < 0.001$; $F_{treatment \times time\ (4,\ 90)} = 18.662$, $p < 0.001$. Ipsi: $F_{treatment\ (1,\ 90)} = 0$, $p = 1$; $F_{time\ (4,\ 90)} = 0.563$, $p = 0.69$; $F_{treatment \times time\ (4,\ 90)} = 0.256$, $p = 0.905$. (E) Con: $F_{treatment\ (1,\ 90)} = 1045.843$, $p < 0.001$; $F_{time\ (4,\ 90)} = 199.553$, $p < 0.001$; $F_{treatment \times time\ (4,\ 90)} = 213.138$, $p < 0.001$. Ipsi: $F_{treatment\ (1,\ 90)} = 0.381$, $p = 0.539$; $F_{time\ (4,\ 90)} = 0.759$, $p = 0.555$; $F_{treatment \times time\ (4,\ 90)} = 0.736$, $p = 0.57$. (F) $F_{treatment\ (1,\ 90)} = 396.824$, $p < 0.001$; $F_{time\ (4,\ 90)} = 113.187$, $p < 0.001$; $F_{treatment \times time\ (4,\ 90)} = 104.324$, $p < 0.001$.

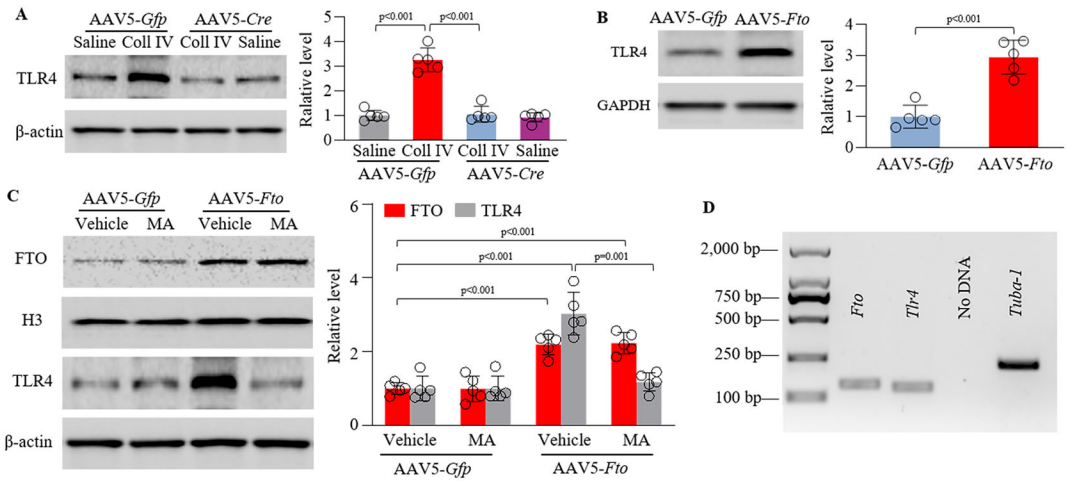

Figure 5.

Increased FTO stabilizes the Coll IV microinjection-induced TLR4 upregulation in the thalamus. (A) Effect of thalamic pre-microinjection of AAV5-*Cre* or AAV5-*Gfp* into unilateral thalamus of *Fto*$^{fl/fl}$ male mice 35 days before Coll IV or saline microinjection into the same regions on the expression of TLR4 protien in thalamus. n = 5 mice/group. Statistical significance was calculated with two-way ANOVA (treatment × model) followed by post hoc Tukey test. $F_{treatment\ (1,\ 16)} = 65.941$, $p < 0.001$; $F_{model\ (1,\ 16)} = 60.536$, $p < 0.001$; $F_{treatment \times treatment\ (1,\ 16)} = 52.71$, $p < 0.001$. (B) Level of TLR4 protein in the ipsilateral thalamus 5 weeks after microinjection of AAV5-*Fto* or AAV5-*Gfp* into unilateral thalamus. n = 5 mice/treatment. Statistical significance was calculated with two-tailed unpaired Student's *t*-test. $t_{(8)} = -6.442$. (C) Effect of intraperitoneal administration of meclofenamic acid (MA; 10 mg/kg) once daily for 5 days starting 35 days post-viral microinjection on the levels of FTO and TLR4 proteins in the ipsilateral thalamus of naïve male mice 40 days after microinjection. n = 5 mice/treatment. Statistical significance was calculated with two-way ANOVA (treatment × model) followed by post hoc Tukey test. FTO: $F_{model\ (1,\ 16)} = 98.045$, $p < 0.001$; $F_{treatment\ (1,\ 16)} = 0.015$, $p = 0.904$; $F_{treatment \times treatment\ (1,\ 16)} = 0.038$, $p = 0.848$. TLR4: $F_{model\ (1,\ 16)} = 38.893$, $p < 0.001$; $F_{treatment\ (1,\ 16)} = 27.386$, $p < 0.001$; $F_{treatment \times model\ (1,\ 16)} = 27.313$, $p < 0.001$. (D) Co-expression of *Fto* mRNA and *Tlr4* mRNA in individual thalamic neurons. n = 3 mice. *Tuba-1a* was used a positive control.

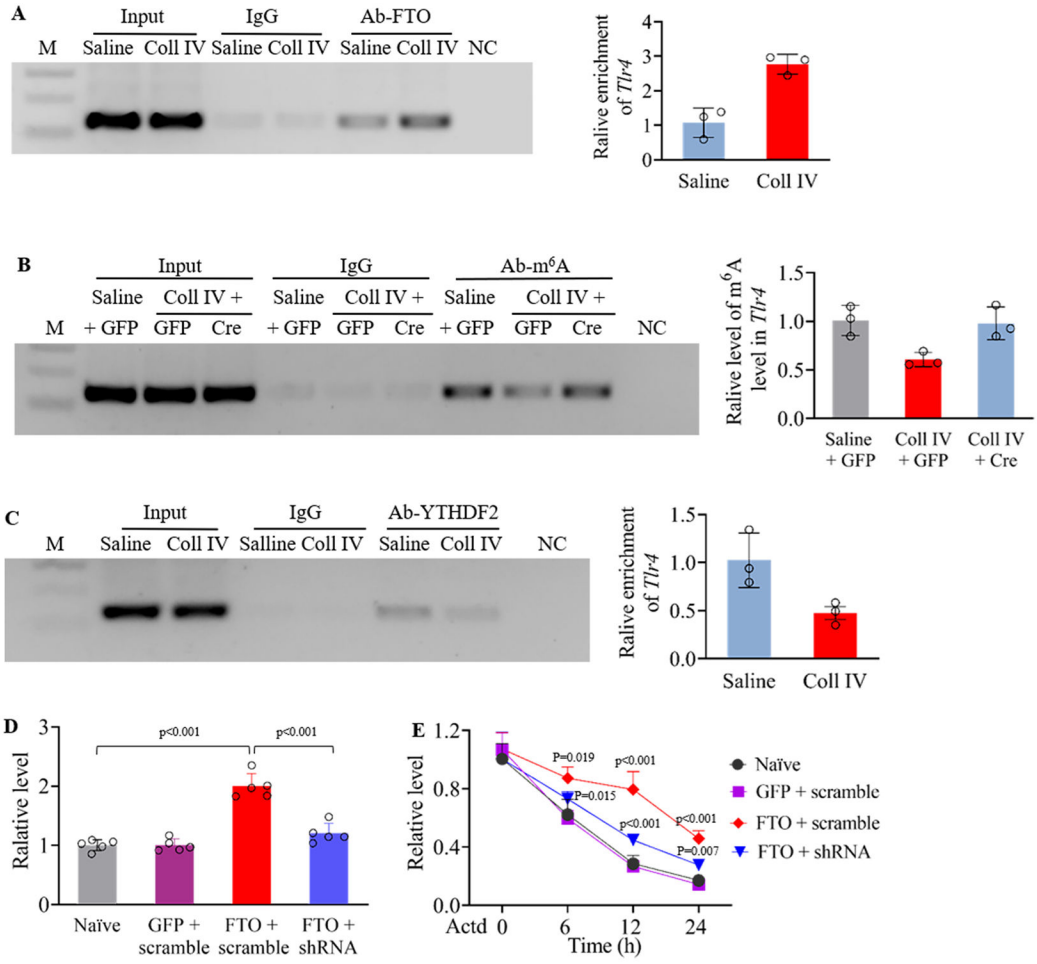

Figure 6.

Increased FTO is responsible for a loss of m^{6}A sites in *Tlr4* mRNA from the thalamus after Coll IV microinjection. M: ladder marker. NC: negative control (distilled H_2O). Input: total purified *Tlr4* mRNA fragments from the ipsilateral thalamus. (A) Level of *Tlr4* mRNA fragment immunoprecipitated by rabbit anti-FTO in the ipsilateral thalamus 7 days after Coll IV or saline microinjection. n = 3 independent repeats (10 mice/repeat)/group. Saline group: 1.07 ± 0.429. Coll IV group: 2.766 ± 0.29. (B) Level of m^{6}A in the *Tlr4* mRNA fragment immunoprecipitated by rabbit anti-m^{6}A in the ipsilateral thalamus of male *Fto*$^{fl/fl}$ mice pre-microinjected with AAV5-*Cre* (Cre) or AAV5-*Gfp* (GFP) 7 days after Coll IV or saline microinjection. n = 3 independent repeats (10 mice/repeat)/group. Saline plus AAV5-*Gfp* group: 1.008 ± 0.155. Coll IV plus AAV5-*Gfp* group: 0.605 ± 0.074. Coll IV plus AAV5-*Cre* group: 0.978 ± 0.169. (C) Level of *Tlr4* mRNA fragment immunoprecipitated by rabbit anti-YTHDF2 in the ipsilateral thalamus 7 days after Coll IV or saline microinjection. n = 3 independent repeats (10 mice/repeat)/group. Saline group: 1.025 ± 0.283. Coll IV group: 0.475 ± 0.117. (D) Level of *Fto* mRNA in CAD cells transfected by the vectors expressing FTO, GFP or FTO shRNA 24 h after transfection. n = 5 independent repeats/treatment. Statistical significance was calculated with one-way ANOVA followed by *post hoc* Tukey test. $F_{(3, 16)} = 49.569$, $p < 0.001$. (E) Expression of *Tlr4* mRNA in the CAD cells transfected by the vectors as shown in D and treated with actinomycin D (ActD; 5

μg/ml) for the indicated times. n = 5 independent repeats/treatment/time point. The *p* values on top of red diamonds indicate a difference from the baseline (0 h) of the corresponding group. The *p* values on top of blue triangles indicate a difference between the FTO plus scrambled siRNA group and FTO plus FTO siRNA group at the corresponding time points. Statistical significance was calculated with two-way ANOVA (treatment × time) followed by *post hoc* Tukey test. $F_{treatment\ (3,\ 64)} = 47.694$, $p < 0.001$; $F_{time\ (3,\ 64)} = 308.162$, $p < 0.001$; $F_{treatment \times time\ (9,\ 64)} = 6.805$, $p < 0.001$.